

Bright red light-emitting devices based on a novel europium complex doped into polyvinylcarbazole†

Yong Zhang, Chun Li, Huahong Shi, Bin Du, Wei Yang and Yong Cao*

Received (in Durham, UK) 4th December 2006, Accepted 22nd February 2007

First published as an Advance Article on the web 19th March 2007

DOI: 10.1039/b617612g

The complex (1,10-phenanthroline)tris[4,4,4-trifluoro-1-(9,9-dihexylfluoren-2-yl)-1,3-butanedione] europium(III), Eu(FTA)₃Phen, was synthesized. Devices based on the complex doped into a PVK:PBD host as emitter were fabricated and showed good performance. A double-layer device with a device configuration of ITO/PEDOT:PSS (150 nm)/PVK:PBD:Eu(FTA)₃Phen (80 nm)/Ba (4 nm)/Al (200 nm) with 0.2 wt% Eu(FTA)₃Phen doping concentration emitted a sharp red emission due to the europium(III) ion at 612 nm. The device showed a highest luminance of 114 cd m⁻² at 12.3 V, a maximum external quantum efficiency of 0.41% and a maximum luminance efficiency of 0.44 cd A⁻¹ at 7.5 V. Furthermore, after inserting a TPBI layer, the device performance was greatly enhanced. At 1% w/w Eu(FTA)₃Phen doping concentration, a highest luminance of 465 cd m⁻² at 16.7 V, maximum external quantum efficiency of 4.28% and maximum luminance efficiency of 4.60 cd A⁻¹ at 9.0 V were obtained from a triple-layer device with a configuration of ITO/PEDOT:PSS (150 nm)/PVK:PBD:1 wt% Eu(FTA)₃Phen (80 nm)/TPBI (45 nm)/Ba (4 nm)/Al (200 nm).

Introduction

Europium complexes showing organic electroluminescence (EL) are of great interest and considered as promising candidates for flat-panel display applications.^{1,2} Various europium complexes have been used in organic EL devices since the first report by Kido *et al.*¹ The emission from europium complexes results from electronic transitions between the 4f energy levels (⁵D₀–⁷F_J (*J* = 0, 1, 2, 3, 4)), therefore changing the ligands in the europium complex will have little effect on the characteristic emission of the europium ion.² Commonly, organic light-emitting devices (OLEDs) based on europium complexes as the emitting layer are fabricated by vacuum deposition.³ Recently, more and more studies have utilized spin-coating techniques to fabricate polymer light-emitting devices (PLEDs) of europium complexes blended into conjugated or non-conjugated polymers.⁴ However, devices formed by this method have exhibited low EL efficiencies compared to devices formed by the vacuum deposition method. One of the reasons for the low efficiencies is a limited choice of polymer hosts for europium complexes. Until now, only a few polymers, such as polyvinylcarbazole (PVK)^{4c} and poly(2-(6-cyano-6-methyl)heptyloxy-1,4-phenylene) (CN-PPP),^{4a} have been selected as polymer hosts for Eu complexes due to a good match between the triplet energy levels of the polymer host and guest, and good overlap between the emission of the polymer host and

the absorption of the guest complex. In this regard, the design and synthesis of new Eu complexes which show good energy level matches and phase compatibility with the existing host materials is an important approach.

In this paper, we report the design and synthesis of a novel europium complex with ligands based on an alkyl-substituted fluorene unit, which has a larger conjugation length than a benzene unit, and the EL properties of devices fabricated from the europium complex as dopant and PVK as host were also investigated. To our best knowledge, there are only a few reports of the synthesis of fluorene-based europium complexes⁵ and no reports have focused on their electroluminescent properties in PLEDs.

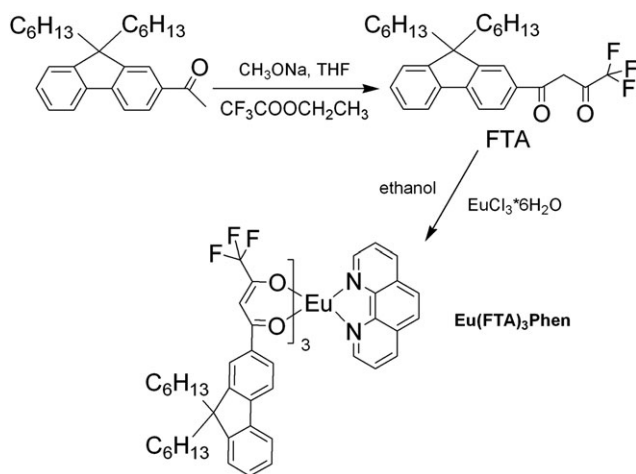
Results and discussion

The general synthetic route to the fluorene-based europium complex is shown in Scheme 1 and the detailed synthetic procedures are presented in the Electronic Supplementary Information (ESI†). Alkylation of 2-acetylfluorene with 1-bromohexane in DMSO–NaOH afforded 9,9-dihexyl-2-acetylfluorene in 71% yield. The β-diketone FTA was prepared by the reaction of 9,9-dihexyl-2-acetylfluorene and trifluoroacetic acetate under Claisen condensation⁶ conditions in a yield of 74%. The target europium complex Eu(FTA)₃Phen was synthesized from FTA, 1,10-phenanthroline and EuCl₃·6H₂O following the literature method.⁷ The structures of the compounds were confirmed by NMR and mass spectroscopy. The elemental analysis of Eu(FTA)₃phen was also measured. All characterization results are available in the ESI.

Both the thermal properties and cyclic voltammetry (CV) of Eu(FTA)₃Phen were investigated. The melting point (*T*_m) of Eu(FTA)₃Phen was found to be 126 °C. The low *T*_m is due to the introduction of two long flexible hexyl groups at the

Institute of Polymer Optoelectronic Materials and Devices, Key Laboratory of Special Functional Materials of Ministry of Education, South China University of Technology, Guangzhou, 510640, P. R. China. E-mail: poycao@scut.edu.cn; Fax: +86 20-87110606; Tel: +86 20-87114609

† Electronic supplementary information (ESI) available: General procedure for device fabrication and characterization and detailed synthetic procedures for all compounds. See DOI: 10.1039/b617612g



Scheme 1 The synthetic route to $\text{Eu}(\text{FTA})_3\text{Phen}$.

9-position of the fluorene unit. The glass transition temperature (T_g) of $\text{Eu}(\text{FTA})_3\text{Phen}$ was found to be 64 °C. This indicates that introduction of the flexible alkyl chain substantially reduces the T_g of the $\text{Eu}(\text{FTA})_3\text{Phen}$ complex. The decomposition temperature (T_d) of $\text{Eu}(\text{FTA})_3\text{Phen}$ was found to be 326 °C (5% weight loss, Fig. 1), suggesting improved thermal stability compared with that of (1,10-phenanthroline) tris[4,4,4-trifluoro-1-phenyl-1,3-butanedione]europium(III) $\text{Eu}(\text{TPD})_3\text{Phen}$ ($T_d = 318$ °C).^{2b} The cyclic voltammetry (CV) experiment was conducted at a $\text{Eu}(\text{FTA})_3\text{Phen}$ concentration of 2×10^{-4} M in dichloromethane solution containing 0.1 M tetrabutylammonium hexafluorophosphate (Bu_4NPF_6) with a platinum working electrode and a saturated calomel electrode as the reference electrode at a scan rate of 50 mV s⁻¹. The HOMO and LUMO levels were estimated from the redox onset following an empirical formula.⁸ The values of the HOMO and LUMO for $\text{Eu}(\text{FTA})_3\text{Phen}$ are estimated as -6.07 eV and -2.76 eV, respectively.

Fig. 2 presents the UV-Vis absorption and PL spectra of $\text{Eu}(\text{FTA})_3\text{phen}$ in dilute THF solution (about 1×10^{-6} M) and in PMMA (0.2 wt%). In the UV-Vis absorption spectrum, the λ_{max} values of $\text{Eu}(\text{FTA})_3\text{phen}$ in THF and PMMA thin

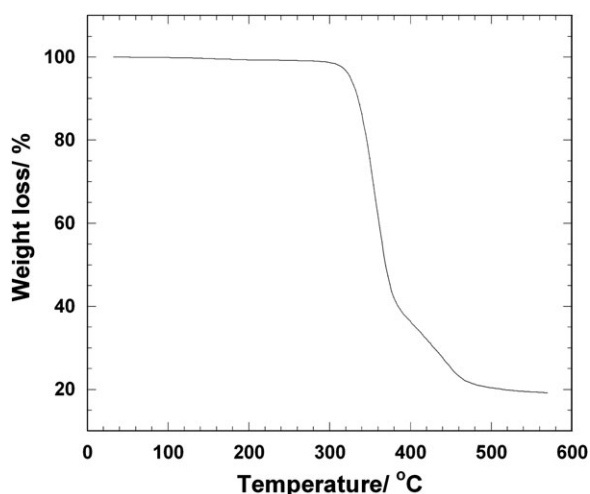


Fig. 1 The TGA curve of $\text{Eu}(\text{FTA})_3\text{Phen}$.

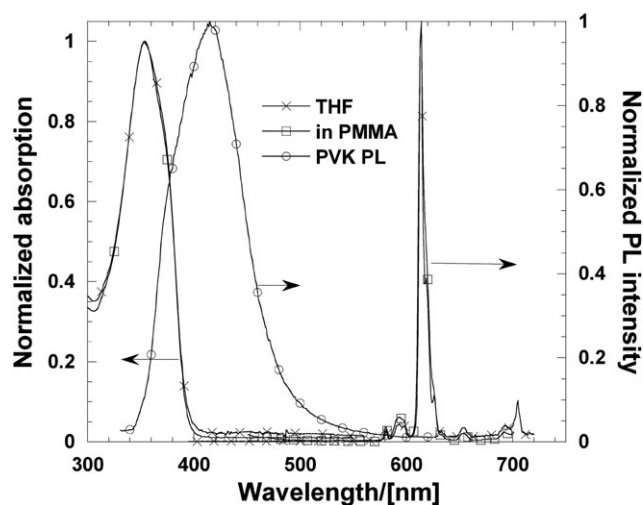


Fig. 2 The UV-Vis spectra and PL spectra of $\text{Eu}(\text{FTA})_3\text{Phen}$ in solution and in PMMA (0.2 wt%) and PL spectrum of PVK in thin film.

film are 354 and 353 nm, respectively, which are assigned to the $\pi-\pi^*$ transition. The 30 nm red-shift compared with the absorption peak of $\text{Eu}(\text{TPD})_3\text{phen}$ (325 nm) is due to the incorporation of the fluorene moiety resulting in a significant increase in conjugation of the ligand.^{2b} The PL spectra (Fig. 2) of $\text{Eu}(\text{FTA})_3\text{phen}$ in both solution and thin film show the characteristic sharp red emission of the Eu ion with almost no difference in peak positions. The five luminescence bands centered at 581, 593, 614, 654 and 705 nm are attributed to the $^5\text{D}_0-^7\text{F}_0$, $^5\text{D}_0-^7\text{F}_1$, $^5\text{D}_0-^7\text{F}_2$, $^5\text{D}_0-^7\text{F}_3$ and $^5\text{D}_0-^7\text{F}_4$ transitions of Eu ion, respectively. The PL quantum yield (PLQY) of $\text{Eu}(\text{FTA})_3\text{phen}$ in dichloromethane was measured with coumarin-1 ($\Phi_r = 60\%$ in ethanol solution) as reference.⁹ The PLQY value is 89% which is significant higher than that of $\text{Eu}(\text{TPD})_3\text{phen}$ (28%).^{2b} Significantly enhanced PL efficiency for $\text{Eu}(\text{FTA})_3\text{phen}$ complex in solution can be attributed to that incorporation of voluminous dihexylfluorene substitution into β -diketonate ligand effectively suppressed the concentration quenching of Eu ions.

PVK was used as the host for the europium complex in this study due to its good hole-transporting properties. At the same time, we blended PVK with 30 wt% of 2-(4-biphenyl)-5-(4-*tert*-butylphenyl)-1,3,4-oxadiazole (PBD), which is a good electron-transporting material in order to get a more balanced electron and hole current.

As shown in Fig. 2, the absorption spectrum of $\text{Eu}(\text{FTA})_3\text{Phen}$ has a large overlap with the PL spectrum of the PVK host. The large spectral overlap is due to the large red-shift of the absorption spectrum of $\text{Eu}(\text{FTA})_3\text{Phen}$ compared with other europium complexes reported so far by many groups.^{1b,2b,3a} Therefore, efficient energy transfer from the PVK host to $\text{Eu}(\text{FTA})_3\text{Phen}$ could be expected to occur via the Förster process.¹⁰ To investigate the efficiency of Förster energy transfer, films containing PVK:30 wt% PBD with varying concentrations of $\text{Eu}(\text{FTA})_3\text{Phen}$ were prepared and examined by optical excitation at 325 nm. Fig. 3 shows the PL spectra of various doping concentrations of $\text{Eu}(\text{FTA})_3\text{Phen}$ in PVK:30 wt% PBD films. The PL profile contains two main

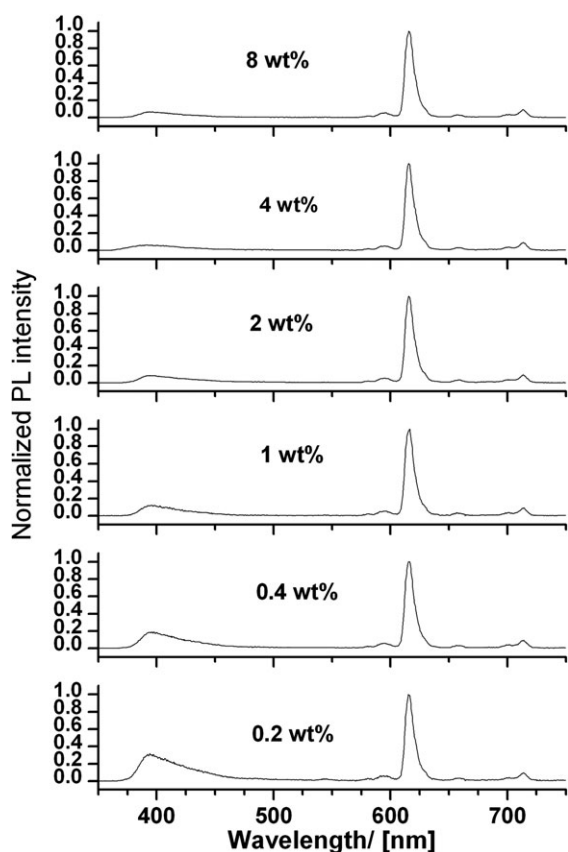


Fig. 3 The PL spectra of $\text{Eu}(\text{FTA})_3\text{Phen}$ doped into PVK:30 wt% PBD at various concentrations.

peaks: one is centered at 430 nm which can be assigned to PVK:PBD emission and the other is the characteristic sharp emission band at 614 nm from $\text{Eu}(\text{FTA})_3\text{Phen}$ emission. The intensity at around 430 nm due to PVK emission was reduced significantly along with the increase in $\text{Eu}(\text{FTA})_3\text{Phen}$ emission (614 nm) with an increase in the concentration of $\text{Eu}(\text{FTA})_3\text{Phen}$ complex indicating efficient Förster energy transfer from the PVK:PBD host to the Eu complex guest.⁴ When the doping concentration of $\text{Eu}(\text{FTA})_3\text{Phen}$ in the PVK increased to 8 wt%, the energy transfer became almost complete showing traces of emission from the PVK:PBD host. At low doping concentrations, Förster energy transfer from the polymer host to $\text{Eu}(\text{FTA})_3\text{Phen}$ is incomplete because of the large average distance from a polymer chain to $\text{Eu}(\text{FTA})_3\text{Phen}$.

To investigate the EL properties, double-layer devices with the configuration of indium tin oxide (ITO)/PEDOT:PSS (150 nm)/PVK:30 wt% PBD: x wt% $\text{Eu}(\text{FTA})_3\text{Phen}$ (80 nm)/Ba (4 nm)/Al (200 nm) were fabricated. The EL spectra of the device at 0.4 wt% doping concentration at different voltages show the characteristic sharp red europium emission peak at 614 nm, the intensity of which increases with applied voltage (Fig. 4a). At 10 V, the EL spectrum was almost completely dominated by the europium ion emission, which is consistent with charge trapping of the europium complex, rather than Förster transfer, as the dominant mechanism in OLEDs.¹¹ With further increasing the voltage in the device, the exciplex emission from PVK:PBD could be observed. This phenom-

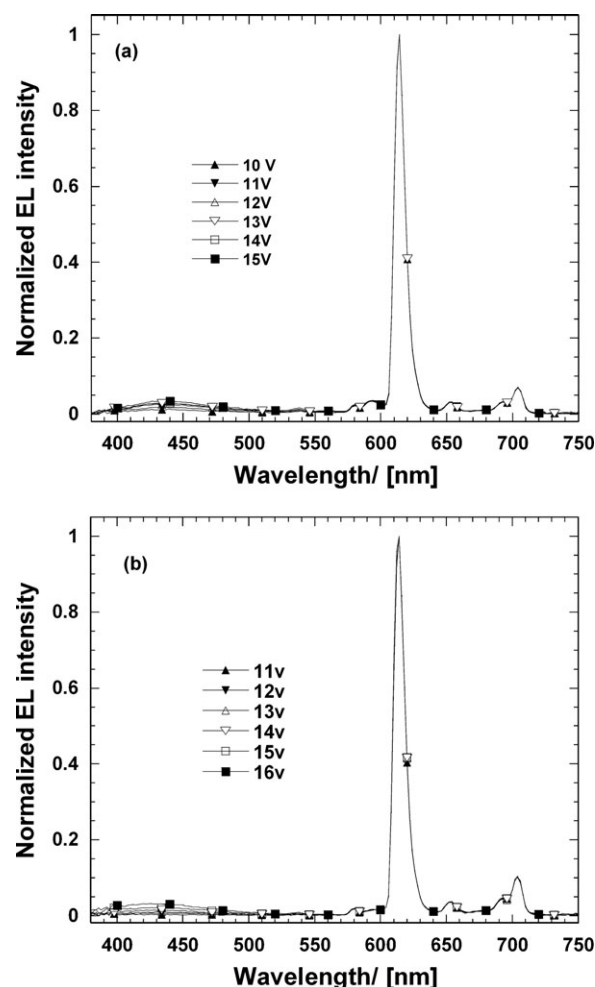


Fig. 4 The EL spectra of the double- (a) and triple-layer (b) devices at different applied voltages at 0.4 wt% doping concentration.

on has been reported previously for doped devices in the literature.¹²

Device efficiencies varied with $\text{Eu}(\text{FTA})_3\text{Phen}$ doping concentration. The maximum external quantum efficiency (EQE) of 0.41% was obtained for the device with 0.2 wt% doping concentration with a maximum luminance efficiency of 0.44 cd A^{-1} at 7.5 V. The highest brightness reached was 114 cd m^{-2} at 12.3 V. This is among the best performances for double layer devices based on europium complexes as dopant and PVK as host in PLEDs.^{4a,b,13} The current density (J)–voltage (V), luminance (L)– V and J –luminance efficiency (LE) curves at various $\text{Eu}(\text{FTA})_3\text{Phen}$ doping concentrations are presented in Fig. 5. As reported previously,^{3a} EL efficiency of phosphorescent devices typically decreases significantly with increasing current density due to increased triplet–triplet annihilation at high current density^{3a} and field-induced quenching effects.¹⁴ For the double-layer devices, as shown in Fig. 5b the device efficiency showed a moderate drop with increasing current density. It is interesting to note that in contrast to most previous reports,¹⁵ devices with high doping concentrations of complexes showed much less current density dependence than those with low doping concentration. It is not clear at this point in the experiment how to understand the

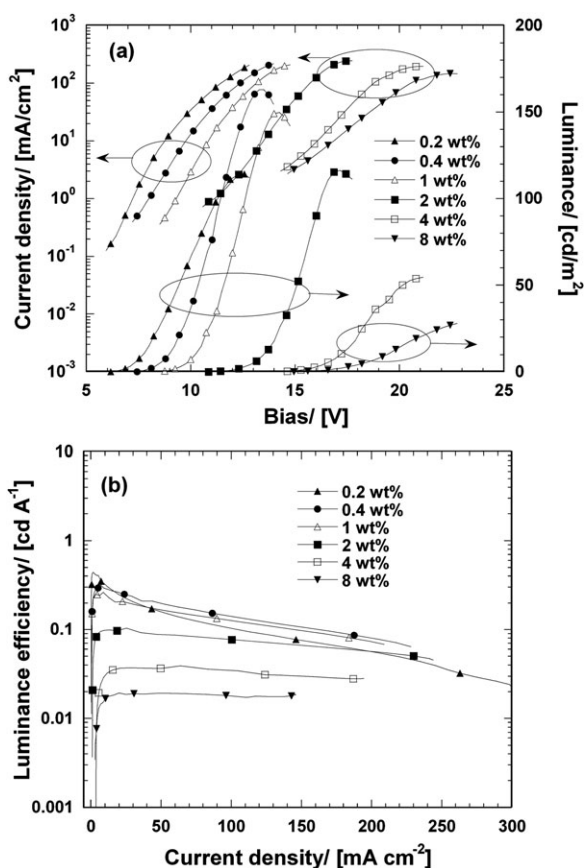


Fig. 5 The J - V - L (a) and LE - J curves (b) of the double-layer devices (device structure: ITO/PEDOT:PSS (150 nm)/PVK:30 wt% PBD: x wt% Eu(FTA)₃Phen (80 nm)/Ba (4 nm)/Al (200 nm)) at various Eu(FTA)₃Phen doping concentrations.

observation and related studies are in progress. The detailed device performance is summarized in Table 1.

To achieve high device performance, balanced charge injection and transport is one of the most important factors.

Table 1 The maximum device performance at various Eu(FTA)₃Phen doping concentrations of double- and triple-layer device structures

Device structure ^a	V_{th}^b/V	Max EQE (%)	Max LE/cd A ⁻¹	Max $L/cd m^{-2}$
0.2 wt% Eu(FTA) ₃ phen	6.6	0.41	0.44	114
0.2 wt% Eu(FTA) ₃ phen/TPBI	6.4	3.00	3.23	281
0.4 wt% Eu(FTA) ₃ phen	7.7	0.30	0.32	163
0.4 wt% Eu(FTA) ₃ phen/TPBI	7.1	4.08	4.40	450
1 wt% Eu(FTA) ₃ phen	9.0	0.25	0.26	150
1 wt% Eu(FTA) ₃ phen/TPBI	8.1	4.28	4.60	465
2 wt% Eu(FTA) ₃ phen	11.8	0.10	0.10	116
2 wt% Eu(FTA) ₃ phen/TPBI	9.5	3.30	3.55	526
4 wt% Eu(FTA) ₃ phen	15.3	0.04	0.04	55
4 wt% Eu(FTA) ₃ phen/TPBI	10.1	3.83	4.12	475
8 wt% Eu(FTA) ₃ phen	16.3	0.02	0.02	28
8 wt% Eu(FTA) ₃ phen/TPBI	9.6	2.50	2.69	444

^a The device structures are ITO/PEDOT:PSS (150 nm)/PVK:30 wt% PBD: x wt% Eu(FTA)₃Phen (80 nm)/(or TPBI 45 nm)/Ba (4 nm)/Al (200 nm). ^b Voltage when luminance reaches 1 cd m⁻².

Typically a much higher hole current was observed for devices from the europium complex doped into a PVK host resulting in low efficiency due to the high hole mobility of the PVK host.¹⁶ As reported previously, in order to reduce hole current and improve the charge balance, 2,9-dimethyl-4,7-diphenyl-1,10-phenanthroline (BCP) is commonly used as an electron injection (EIL)/hole-blocking layer (HBL) for europium complexes/small molecule host devices.^{3a,d,4c} In this work, we found out that 1,3,5-tris(2-*N*-phenylbenzimidazolyl) benzene (TPBI) serves as good electron injection layer (rather than HBL) for Eu complex/PVK devices. Triple-layer devices with the configuration ITO/PEDOT:PSS (150 nm)/PVK:30 wt% PBD: x wt% Eu(FTA)₃Phen (80 nm)/TPBI (45 nm)/Ba (4 nm)/Al (200 nm) were fabricated. The devices show a remarkable enhancement, more than ten-fold, in EL efficiencies after inserting a TPBI layer compared to double-layer devices without a TPBI layer. The EL spectra of devices with 0.4 wt% doping concentration at different voltages (Fig. 4b) showed almost identical spectra to those of the double devices. Table 1 shows the EL performances of the devices with various Eu(FTA)₃Phen doping concentrations. The device with 1 wt% doping concentration gave the best EL performance. The maximum EQE is 4.28%, corresponding to luminance and power efficiencies of 4.60 cd A⁻¹ and 1.67 lm W⁻¹,

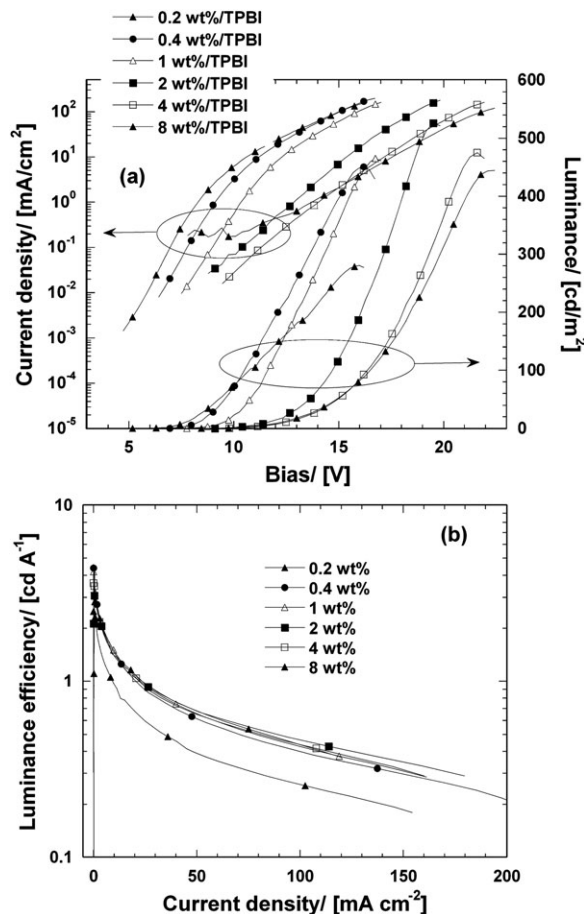


Fig. 6 The J - V - L (a) and LE - J (b) curves of the triple-layer devices (device structure: ITO/PEDOT:PSS (150 nm)/PVK:30 wt% PBD: x wt% Eu(FTA)₃Phen (80 nm)/TPBI (45 nm)/Ba (4 nm)/Al (200 nm)) at various Eu(FTA)₃Phen doping concentrations.

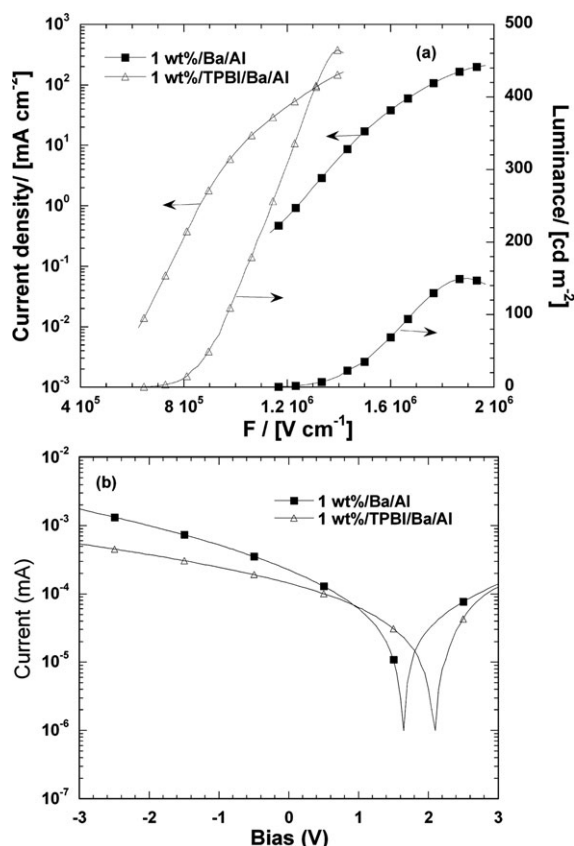


Fig. 7 The compared J - F - L curves (a) and photovoltaic characteristics (b) of the double- and triple-layer devices with 1 wt% Eu(FTA)₃Phen doping concentration.

respectively. The turn-on voltage reduces to 8.1 V compared with 9.0 V for the corresponding double-layer device. The maximum brightness reaches 465 cd m⁻² at 16.7 V. To our best knowledge, this is the best EL efficiency based on a europium complex in PLED by spin casting technology reported so far. Fig. 6 presents the J - V - L and J - LE curves at various Eu(FTA)₃Phen doping concentrations.

Fig. 7a compares the J - F - L curves at 1 wt% Eu(FTA)₃Phen doping concentration for double- and triple-layer devices. At the same field strength, the device with a TPBI layer has a much higher current density and higher luminance than that of the device without a TPBI layer. This indicates that device has a more balanced electron and hole current in the emitting layer after inserting a TPBI layer mainly due to improved electron injection. As shown in Table 1, the turn-on voltage (defined as voltage at 1 cd m⁻²) was significantly reduced by having a TPBI layer, especially for the devices with high Eu(FTA)₃Phen doping concentrations, for instance at 4 wt% doping concentration the turn-on voltage reduced to 10.1 V with a TPBI layer from 15.3 V without a TPBI layer. In order to understand the mechanism of the reduction of operating voltage after insertion of a TPBI layer, photovoltaic measurements were carried out to determine the built-in potential across the devices. Fig. 7b compares photocurrent- V curves and the open-circuit voltage (V_{oc}) of the double- and triple-layer devices at 1 wt% Eu(FTA)₃Phen under white-light illumination (78 mW cm⁻²). As reported previously,¹⁷ photovoltaic

measurements might provide a simple measurement of built-in potential (V_{bi}). At zero applied voltage the OLED acts as a photovoltaic cell, where photo-generated charges drift under the influence of V_{bi} to produce a photocurrent as a first approximation, the voltage when the photocurrent has been completely compensated by applying a bias is equal to the open circuit voltage (V_{oc}). The open-circuit voltage was approximately 1.6 V in the double-layer device and shifted to 2.1 V for the triple-layer device. Since the anode interface was kept the same in both double- and triple-layer devices, a significant increase in the built-in potential indicates the reduction barrier height in the cathode interface which leads to a significant reduction of the turn-on voltage and improvement of the device efficiency due to dramatically increasing electron injection. We note that device efficiency increased more significantly after insertion of TPBI for the blend with the higher Eu complex concentration. The EQE for devices with 4 wt% and 8 wt% dopant concentrations increased more than one hundred-fold compared to that without a TPBI layer. At this stage in the experiment, it is not clear why TPBI could make such a difference for devices with different dopant concentrations. Further experiments are planned to elucidate this problem.

Conclusions

In summary, we synthesized a novel dihexyl-substituted fluorene-based europium complex, Eu(FTA)₃Phen. The EL devices fabricated from the Eu(FTA)₃Phen complex doped into PVK:PBD host as the emitting layer show good performance. After inserting a thin layer of TPBI, the device performance was greatly improved up to a maximum EQE of 4.28% and luminance efficiency of 4.60 cd A⁻¹ which is the highest EQE reported so far for devices based on europium complexes in PLEDs. The mechanism of the enhancement of device efficiency by insertion of a TPBI layer was investigated by photovoltaic measurement. A significant increase in built-in potential indicates a reduction in barrier height in the cathode interface which leads to a reduction of the turn-on voltage and improvement of device efficiency as a result of the increase in electron injection.

Acknowledgements

The authors are deeply grateful to the National Natural Science Foundation of China (Project No. 50433030 and U0634003) and the MOST National Research Project (No. 2002CB613403) for financial support.

References

- (a) J. Kido, K. Nagai and Y. Ohashi, *Chem. Lett.*, 1990, 657; (b) J. Kido and Y. Okamoto, *Chem. Rev.*, 2002, **102**, 2357.
- (a) X. H. Zhu, L. H. Wang, J. Ru, W. Huang, J. F. Fang and D. G. Ma, *J. Mater. Chem.*, 2004, **14**, 2732; (b) Y. Zhang, H. H. Shi, Y. Ke and Y. Cao, *J. Lumin.*, 2007, **124**, 51.
- (a) C. Adachi, M. A. Baldo and S. R. Forrest, *J. Appl. Phys.*, 2000, **87**, 8049; (b) M. Shi, F. Y. Li, T. Yi, D. Q. Zhang, H. M. Hu and C. H. Huang, *Inorg. Chem.*, 2005, **44**, 8929; (c) H. Xu, L. H. Wang, X. H. Zhu, K. Yin, G. Y. Zhong, X. Y. Hou and W. Huang, *J. Phys. Chem. B*, 2006, **110**, 3023; (d) T. W. Canzler and J. Kido, *Org. Electron.*, 2006, **7**, 29.

- 4 (a) M. D. McGehee, T. Bergstedt, C. Zhang, A. P. Saab, M. B. O'Regan, G. C. Bazan, V. I. Srdanov and A. J. Heeger, *Adv. Mater.*, 1999, **11**, 1349; (b) M. R. Robinson, J. C. Ostrowski, G. C. Bazan and M. D. McGehee, *Adv. Mater.*, 2003, **15**, 1547; (c) N. A. H. Male, O. V. Salata and V. Christou, *Synth. Met.*, 2002, **126**, 7.
- 5 (a) M. Uekawa, Y. Miyamoto, H. Ikeda, K. Kaifu and T. Nakaya, *Synth. Met.*, 1997, **91**, 259; (b) M. Uekawa, Y. Miyamoto, H. Ikeda, K. Kaifu and T. Nakaya, *Bull. Chem. Soc. Jpn.*, 1998, **71**, 2253; (c) R. G. Charles and E. P. Riedel, *J. Inorg. Nucl. Chem.*, 1967, **29**, 715.
- 6 T. D. Penning, J. J. Talley, S. R. Bertenshaw, J. S. Carter, P. W. Collins, S. Docter, M. J. Graneto, L. F. Lee, J. W. Malecha, J. M. Miyashiro, R. S. Rogers, D. J. Rogier, S. S. Yu, G. D. Anderson, E. G. Burton, J. N. Cogburn, S. A. Gregory, C. M. Koboldt, W. E. Perkins, K. Seibert, A. W. Veenhuizen, Y. Y. Zhang and P. C. Isakson, *J. Med. Chem.*, 1997, **40**, 1347.
- 7 (a) L. R. Melby, N. J. Rose, E. Abramson and J. C. Caris, *J. Am. Chem. Soc.*, 1964, **86**, 5117; (b) K. Okada, Y. F. Wang, T. M. Chen, M. Kitamura, T. Nakaya and H. Inoue, *J. Mater. Chem.*, 1999, **9**, 3023.
- 8 Y. T. Cui, X. J. Zhang and S. A. Jenekhe, *Macromolecules*, 1999, **32**, 3824.
- 9 Y. L. Chen, C. Sinha, I. C. Chen, K. L. Liu, Y. Chi, J. K. Yu, P. T. Chou and T. H. Lu, *Chem. Commun.*, 2003, 3046.
- 10 T. Förster, *Discuss. Faraday Soc.*, 1959, **27**, 7.
- 11 (a) X. Gong, J. C. Ostrowski, D. Moses, G. C. Bazan and A. J. Heeger, *Adv. Funct. Mater.*, 2003, **13**, 439; (b) X. Gong, S. H. Lim, J. C. Ostrowski, D. Moses, C. J. Bardeen and G. C. Bazan, *J. Appl. Phys.*, 2004, **95**, 948.
- 12 (a) P. P. Sun, J. P. Duan, H. T. Shih and C. H. Cheng, *Appl. Phys. Lett.*, 2002, **81**, 792; (b) C. Liang, W. Li, Z. Hong, X. Liu, J. Peng, L. Liu, Z. Lu, M. Xie, Z. Liu, J. Yu and D. Zhao, *Synth. Met.*, 1997, **91**, 151.
- 13 A. O'Riordan, E. O'Connor, S. Moynihan, X. Llinares, R. Van Deun, P. Fias, P. Nockemann, K. Binnemans and G. Redmond, *Thin Solid Films*, 2005, **491**, 264.
- 14 J. Kalinowski, W. Stampor, J. Mężyk, M. Cocchi, D. Virgili, V. Fattori and P. Di Marco, *Phys. Rev. B: Condens. Matter*, 2002, **66**, 235321.
- 15 J. X. Jiang, Y. H. Xu, W. Yang, R. Guan, Z. Q. Liu, H. Y. Zhen and Y. Cao, *Adv. Mater.*, 2006, **18**, 1769.
- 16 A. Baba, K. Onishi, W. Knoll and R. C. Advincula, *J. Phys. Chem. B*, 2004, **108**, 18949.
- 17 G. Yu, C. Zhang and A. J. Heeger, *Appl. Phys. Lett.*, 1994, **64**, 1540.